Computer Methods in Applied Mechanics and Engineering 431 (2024) 117287

Contents lists available at ScienceDirect

Comput. Methods Appl. Mech. Engrg.

journal homepage: www.elsevier.com/locate/cma

Adaptive methods with C^1 splines for multi-patch surfaces and shells

Cesare Bracco [a], Andrea Farahat [b], Carlotta Giannelli [a,*], Mario Kapl [c], Rafael Vázquez [d]

[a] Dipartimento di Matematica e Informatica "U. Dini", Università degli Studi di Firenze, Florence, Italy
[b] Johann Radon Institute for Computational and Applied Mathematics, Austrian Academy of Sciences, Linz, Austria
[c] Department of Engineering & IT, Carinthia University of Applied Sciences, Villach, Austria
[d] Departamento de Matemática Aplicada and Centro de Investigación y Tecnología Matemática de Galicia (CITMAga), Universidade de Santiago de Compostela, Santiago de Compostela, Spain

ARTICLE INFO

MSC:
65D07
65D17
65N30
65N50

Keywords:
Isogeometric analysis
Adaptivity
Hierarchical splines
C^1 continuity
Multi-patch surfaces
Biharmonic problem
Kirchhoff–Love shells

ABSTRACT

We introduce an adaptive isogeometric method for multi-patch surfaces and Kirchhoff–Love shell structures with hierarchical splines characterized by C^1 continuity across patches. We extend the construction of smooth hierarchical splines from the multi-patch planar setting to analysis suitable G^1 surfaces. The adaptive scheme to solve fourth order partial differential equations is presented in a general framework before showing its application for the numerical solution of the bilaplacian and the Kirchhoff–Love model problems. A selection of numerical examples illustrates the performance of hierarchical adaptivity on different multi-patch surface configurations.

1. Introduction

Isogeometric analysis (IGA) is a framework for the numerical solution of partial differential equations (PDEs), which has raised much interest in recent years, due to the advantages of splines for the description of both the geometry and the discretization spaces of the problem (see, e.g. [1]). A very attractive feature of splines in this context is high smoothness, since it allows to numerically solve high-order PDEs without writing them in mixed form. In particular, C^1 regularity is enough to solve the bilaplacian problem, the Kirchhoff–Love shell or Cahn–Hilliard phase-field model without moving away from their direct formulation. Moreover, choosing spline spaces which allow local refinement, that is, which do not have an underlying tensor-product structure, leads to an increased computational efficiency. The goal of this work is to combine these two features to obtain adaptive isogeometric methods for high-order PDEs in complex geometries.

High smoothness of splines is a property which can be obtained in a straightforward way in geometries having a single-patch description. For complex multi-patch domains, which are described by stitching several patches together, the construction of C^1 spline functions is far from being trivial. The existing techniques can be roughly classified into the so-called weak and strong approach depending on whether the C^1 continuity conditions across the patch interfaces are weakly or strongly enforced. While the weak approach generates functions which are in general just approximately C^1 across the patch interfaces, the strong approach

* Corresponding author.
E-mail addresses: cesare.bracco@unifi.it (C. Bracco), andrea.farahat@ricam.oeaw.ac.at (A. Farahat), carlotta.giannelli@unifi.it (C. Giannelli), m.kapl@fh-kaernten.at (M. Kapl), rafael.vazquez@usc.es (R. Vázquez).

https://doi.org/10.1016/j.cma.2024.117287
Received 17 May 2024; Received in revised form 31 July 2024; Accepted 8 August 2024
Available online 20 August 2024

constructs exactly C^1 functions. We summarize below some of the ideas and main references, and refer to [2] for an in-depth survey and comparison of some of them.

An example of the weak approach is variational coupling, which avoids to directly construct a space of C^1 (or approximately C^1) splines on the domain. This is achieved by weakly enforcing the C^1 continuity across the patch interfaces by a modification of the equations of the problem: this gave rise, for instance, to penalty methods (see, e.g. [3,4]), Nitsche's methods (see, e.g. [5,6]) and mortar methods (see, e.g. [7,8]). In contrast to variational coupling, the methods [9–12] directly generate basis functions which are approximately C^1, and the jump on the first derivative decreases when the mesh is refined.

The strong approach has been extensively investigated in recent years, with different solutions according to the type of imposed continuity in the vicinity of extraordinary vertices, where less or more than four patches meet. In [13–15], spline spaces with C^1 continuity everywhere, that is, between all neighboring patches, are defined. This leads to singularities around the extraordinary vertices, which is handled by using a technique inspired by the D-patches introduced in [16]. Closely related to these constructions are subdivision based methods (see e.g. [17–19]). Alternatively, it is possible to replace the C^1 continuity with G^1 smoothness near extraordinary vertices, as it was done in [20–23]. A further alternative is to use G^1 parameterizations of the geometry, where the C^1 continuity is provided only inside the patches, while G^1 smoothness is obtained on the interfaces, see e.g. [24–26] based on bilinear multi-patch domains, and [27–29] employing more general G^1 multi-patch geometries.

In this paper, we employ a particular class of G^1 multi-patch spline geometries called analysis-suitable G^1 multi-patch parameterizations [30], and we emphasize that any G^1 multi-patch parameterization can be closely approximated by an analysis-suitable G^1 multi-patch geometry (see e.g. [31–33]). The use of these geometries provides the construction of a subspace of the C^1 spline space on the geometry with optimal polynomial reproduction properties, dimension not depending on the parameterization of the single patches, and an explicit expression of the basis for the planar [34] and the surface case [31]. These C^1 spline spaces have been successfully used in isogeometric methods to solve several high-order PDEs on planar multi-patch parameterizations [35] and on multi-patch surfaces, including Kirchhoff–Love shells [31,36]. Closely related to techniques using analysis-suitable G^1 multi-patch geometries are the so-called scaled boundary methods (see [37,38]), which employ multi-patch parameterizations that are analysis-suitable G^1 everywhere except at the scaling centers, where the multi-patch parameterization possesses in each case a singularity.

Adaptive methods for finite elements can recover optimal convergence in case of singular solutions, and their mathematical analysis is now well understood, see for instance [39,40] and references therein. In IGA, different generalizations of B-splines have been introduced to incorporate local refinement and adaptivity, such as T-splines, LR-splines, PHT-splines or hierarchical splines, see the recent survey [41] for an in-depth analysis of T-splines and hierarchical splines, and Section 4.3 of the same paper for discussion of other available approaches. Concerning spaces with C^1 continuity on multi-patch geometries, not many works exist so far. Local refinement combined with C^1 continuity at extraordinary vertices was first studied for T-splines in [42,43] and for subdivision surfaces in [44], but the approximation properties of the spaces were suboptimal around extraordinary vertices. The concept of D-patches mentioned above has been applied to T-splines in [14,45], with local refinement constructed a priori, i.e., without using an error estimator. The same D-patch approach was later combined with hierarchical splines in [46], showing good numerical results, although it has not been proved that the obtained spaces fulfill the requirements of the hierarchical framework. In previous works, we have developed adaptive methods for the C^1 splines on analysis-suitable G^1 parameterizations from [34], by recasting them into the framework of truncated hierarchical splines [47], first for planar two-patch geometries in [48], and later for planar multi-patch geometries in [49]. The latter required to relax the assumption of local linear independence from the hierarchical framework, which was replaced by linear independence of single-level functions on certain regions of the mesh. In the same paper we introduced a refinement algorithm that respect this condition by refining few extra elements in the vicinity of extraordinary vertices. The method was then applied to simulations of phase-field modeling in [50], considering both adaptive refinement and coarsening.

In this paper we extend the construction of the hierarchical C^1 space for planar domains from [49] to the multi-patch surface case. We will show that the C^1 spline space [31] defined on analysis-suitable G^1 multi-patch surfaces satisfies the same properties of linear independence as for the planar case, and the definitions and algorithms in [49] can be applied seamlessly. This allows us to develop adaptive isogeometric schemes to solve high order PDEs on multi-patch surface domains, whose performance will be tested on bilaplacian and Kirchhoff–Love shell formulations.

The paper is organized as follows. Section 2 presents the C^1 splines construction from [31] for analysis-suitable G^1 multi-patch surface domains, in particular highlighting the difference with respect to the planar case. Section 3 recalls the hierarchical construction and its properties, showing how it can be applied to the C^1 multi-patch splines of the previous section, and it provides the description of the refinement scheme which will be employed in our adaptive framework. Section 4 contains the definition of the proposed adaptive isogeometric methods to solve fourth order PDEs on surfaces, and extensive numerical tests for the bilaplacian and Kirchhoff–Love shell problems.

2. C^1 splines on multi-patch surfaces with uniform meshes

The development of the adaptive isogeometric method with C^1 hierarchical splines over a planar multi-patch domain, introduced in [49], was based on the definition of C^1 spline spaces for planar multi-patch domains and for each single level [34]. The extension to the surface case, as studied in this work, requires the use on each level of the C^1 spline space in [31], which generalizes the previous construction to multi-patch non-planar surfaces. These spaces must be defined on a domain described by an analysis-suitable G^1 multi-patch geometry [30]. While the definition of analysis-suitable G^1 multi-patch surfaces is analogous in the planar and non-planar cases, by just considering parameterizations in $\mathbb{R}^2$ or in $\mathbb{R}^3$, the extension of the C^1 multi-patch spline space for planar domains to the C^1 multi-patch spline space for surfaces requires an adaption in the construction of the functions in the vicinity of a vertex. Below, we will briefly present the class of analysis-suitable G^1 multi-patch surfaces, and will then introduce the C^1 isogeometric spline space [31] with a focus on the similarities and differences compared to the planar case.

2.1. Analysis suitable G^1 multi-patch surfaces

Let $\mathbb{S}_p^r$ be the univariate spline space of degree $p \geq 3$ and regularity $1 \leq r \leq p-2$ over the unit interval $[0,1]$ with the internal breakpoints $\frac{j}{k+1}$, $j = 0, 1, \dots, k$, and $k \in \mathbb{N}_0$. We consider a connected multi-patch surface domain $\Omega \subset \mathbb{R}^3$, which is the union of closed quadrilateral surface patches $\Omega^{(i)}$, i.e., $\Omega = \bigcup_{i \in \mathcal{I}_\Omega} \Omega^{(i)}$. We assume that no hanging nodes exist, and that the intersection of any two surface patches $\Omega^{(i_1)}$ and $\Omega^{(i_2)}$, $i_1, i_2 \in \mathcal{I}_\Omega$ with $i_1 \neq i_2$, is either empty, a common vertex or a common inner edge. We denote for the multi-patch surface Ω the inner and boundary edges by $\Sigma^{(i)}$, $i \in \mathcal{I}_\Sigma = \mathcal{I}_\Sigma^\circ \cup \mathcal{I}_\Sigma^\Gamma$, as well as the inner and boundary vertices by $\mathbf{x}^{(i)}$, $i \in \mathcal{I}_\chi = \mathcal{I}_\chi^\circ \cup \mathcal{I}_\chi^\Gamma$, where $\mathcal{I}_\Sigma^\circ$ and $\mathcal{I}_\chi^\circ$ collect the indices of the inner edges and vertices, and $\mathcal{I}_\Sigma^\Gamma$ and $\mathcal{I}_\chi^\Gamma$ collect the indices of the boundary edges and vertices. We further assume that each surface patch $\Omega^{(i)}$, $i \in \mathcal{I}_\Omega$, is the image of a bijective and regular geometry mapping

$$\mathbf{F}^{(i)} : [0,1]^2 \to \Omega^{(i)},$$

with $\mathbf{F}^{(i)} \in (\mathbb{S}_p^r \otimes \mathbb{S}_p^r)^3$, and denote the multi-patch surface parameterization of Ω, which consists of the single surface patch parameterizations $\mathbf{F}^{(i)}$, $i \in \mathcal{I}_\Omega$, as $\mathbf{F}$. The resulting multi-patch surface $\mathbf{F}$ is assumed to be analysis-suitable G^1, which means that for each inner edge $\Sigma^{(i)}$, $i \in \mathcal{I}_\Sigma^\circ$, with $\Sigma^{(i)} \subset \Omega^{(i_0)} \cap \Omega^{(i_1)}$, assuming that $\Sigma^{(i)}$ is parameterized as $\mathbf{F}^{(i_1)}(\xi, 0) = \mathbf{F}^{(i_0)}(0, \xi)$, $\xi \in [0,1]$, there exist linear functions $\alpha^{(i,0)}$, $\alpha^{(i,1)}$, $\beta^{(i,0)}$ and $\beta^{(i,1)}$, with $\alpha^{(i,0)}$ and $\alpha^{(i,1)}$ relatively prime, such that for all $\xi \in [0,1]$

$$\alpha^{(i,0)}(\xi)\alpha^{(i,1)}(\xi) > 0$$

and

$$\alpha^{(i,0)}(\xi)\partial_2 \mathbf{F}^{(i_1)}(\xi,0) + \alpha^{(i,1)}(\xi)\partial_1 \mathbf{F}^{(i_0)}(0,\xi) + (\alpha^{(i,0)}(\xi)\beta^{(i,1)}(\xi) + \alpha^{(i,1)}(\xi)\beta^{(i,0)}(\xi))\partial_2 \mathbf{F}^{(i_0)}(0,\xi) = \mathbf{0},$$

see [30,31] for the details. Note that analysis-suitable G^1 multi-patch surfaces are a particular class of G^1 multi-patch surfaces which allow the design of C^1 isogeometric spline spaces with optimal polynomial reproduction properties for the traces and transversal derivatives along the edges [30,34]. Existing methods for the construction of analysis-suitable G^1 multi-patch surfaces can be found in [31–33].

2.2. C^1 splines on multi-patch surfaces and uniform meshes

As for planar analysis-suitable G^1 multi-patch geometries, the C^1 isogeometric spline space $\mathbb{V}$ with respect to the analysis-suitable G^1 multi-patch surface $\mathbf{F}$ is given as

$$\mathbb{V} = \{\phi \in C^1(\Omega) \ : \ \phi \circ \mathbf{F}^{(i)} \in \mathbb{S}_p^r \otimes \mathbb{S}_p^r, i \in \mathcal{I}_\Omega\}.$$

The associated mesh, i.e., the partition of the domain determined by the knot vectors of the univariate spaces $\mathbb{S}_p^r$, is given by

$$G = \left\{ \mathbf{F}^{(i)}(\hat{Q}) : i \in \mathcal{I}_\Omega, \hat{Q} = \left(\frac{j_1}{k+1}, \frac{j_1+1}{k+1}\right) \times \left(\frac{j_2}{k+1}, \frac{j_2+1}{k+1}\right), \text{ for } j_1, j_2 = 0, \dots, k \right\}. \tag{1}$$

For a function $\phi \in \mathbb{V}$, we define for each inner edge $\Sigma^{(i)}$, $i \in \mathcal{I}_\Sigma^\circ$, with $\Sigma^{(i)} \subset \Omega^{(i_0)} \cap \Omega^{(i_1)}$, assuming that $\Sigma^{(i)}$ is parameterized as $\mathbf{F}^{(i_1)}(\xi, 0) = \mathbf{F}^{(i_0)}(0, \xi)$, $\xi \in [0,1]$, the functions

$$f_0^{(i,i_0)}(0,\xi) = \left(\phi \circ \mathbf{F}^{(i_0)}\right)(0,\xi), \text{ and } f_0^{(i,i_1)}(\xi,0) = \left(\phi \circ \mathbf{F}^{(i_1)}\right)(\xi,0),$$

$$f_1^{(i,i_0)}(0,\xi) = \frac{\partial_1 (\phi \circ \mathbf{F})(0,\xi) + \beta^{(i,i_0)}(\xi)\, \partial_2 (\phi \circ \mathbf{F})(0,\xi)}{\alpha^{(i,i_0)}(\xi)},$$

and

$$f_1^{(i,i_1)}(\xi,0) = \frac{\partial_2 (\phi \circ \mathbf{F})(\xi,0) + \beta^{(i,i_1)}(\xi)\, \partial_1 (\phi \circ \mathbf{F})(\xi,0)}{\alpha^{(i,i_1)}(\xi)}.$$

Then, the space $\mathbb{V}$ can be equivalently represented as

$$\mathbb{V} = \{\phi \in L^2(\Omega) \ : \ \phi \circ \mathbf{F}^{(i)} \in \mathbb{S}_p^r \otimes \mathbb{S}_p^r, i \in \mathcal{I}_\Omega, \text{ and } f_j^{(i,i_0)}(0,\xi) = f_j^{(i,i_1)}(\xi,0), \ \xi \in [0,1], \ j = 0,1, \ i \in \mathcal{I}_\Sigma^\circ\},$$

see [31,36]. Let us denote the equally valued terms $f_j^{(i,i_0)}(0,\xi) = f_j^{(i,i_1)}(\xi,0)$ by $f_j^{(i)}$, $j = 0,1$, where $f_0^{(i)}$ describe the trace, and $f_1^{(i)}$ a specific transversal derivative of ϕ across the inner edge $\Sigma^{(i)}$, see [30]. For each boundary edge $\Sigma^{(i)}$, $i \in \mathcal{I}_\Sigma^\Gamma$, with $\Sigma^{(i)} \subset \Omega^{(i_0)}$, assuming that $\Sigma^{(i)}$ is parameterized as $\mathbf{F}^{(i_0)}(\xi, 0)$, $\xi \in [0,1]$, the functions $f_0^{(i)}$ and $f_1^{(i)}$ can be simply defined as

$$f_0^{(i)}(\xi) = \left(\phi \circ \mathbf{F}^{(i_0)}\right)(0,\xi) \text{ and } f_1^{(i)}(\xi) = \partial_1 \left(\phi \circ \mathbf{F}^{(i_0)}\right)(0,\xi).$$

Instead of the space $\mathbb{V}$, which has a complex structure and whose dimension depends on the parameterization, see [51], we consider the simpler subspace

$$\mathbb{A} = \{\phi \in \mathbb{V} \ : \ f_0^{(j)} \in \mathbb{S}_p^{r+1}, f_1^{(j)} \in \mathbb{S}_{p-1}^r, j \in \mathcal{I}_\Sigma, \text{ and } \phi \in C_T^2(\mathbf{x}^{(i)}), \ i \in \mathcal{I}_\chi\}, \tag{2}$$

where $C^2_T(\mathbf{x}^{(i)})$ means C^2-smooth at the vertex $\mathbf{x}^{(i)}$ with respect to the tangent plane at $\mathbf{x}^{(i)}$. Since $f_0^{(j)} \in \mathbb{S}_p^{r+1}$ and $f_1^{(j)} \in \mathbb{S}_{p-1}^{r}$, for $j \in \mathcal{I}_\Sigma$, the C^1 subspace $\mathbb{A} \subset \mathbb{V}$ possesses the same optimal polynomial reproduction properties for the traces and transversal derivatives along the edges as $\mathbb{V}$, see [30, Theorem 1], and has been introduced in [31] as an extension of the planar construction [34]. The difference to the planar case is that the functions are not C^2-smooth at the vertices with respect to the domain Ω, rather C^2-smooth at the vertices with respect to the corresponding tangent planes. However, by requiring $k \geq \max(0, \frac{5-p}{p-r-1})$, a basis $\boldsymbol{\Phi}$ of $\mathbb{A}$ can be constructed as for the planar case by

$$\boldsymbol{\Phi} = \boldsymbol{\Phi}_\Omega \cup \boldsymbol{\Phi}_\Sigma \cup \boldsymbol{\Phi}_\chi, \quad \text{with} \quad \boldsymbol{\Phi}_\Omega = \bigcup_{i \in \mathcal{I}_\Omega} \boldsymbol{\Phi}_{\Omega^{(i)}}, \quad \boldsymbol{\Phi}_\Sigma = \bigcup_{i \in \mathcal{I}_\Sigma} \boldsymbol{\Phi}_{\Sigma^{(i)}}, \quad \boldsymbol{\Phi}_\chi = \bigcup_{i \in \mathcal{I}_\chi} \boldsymbol{\Phi}_{\mathbf{x}^{(i)}}, \tag{3}$$

which respectively correspond to patch interior basis functions, edge basis functions, and vertex basis functions. The particular set of functions for each geometrical entity (patch, edge or vertex) is given as

$$\boldsymbol{\Phi}_{\Omega^{(i)}} = \left\{ \phi_{\mathbf{j}}^{\Omega^{(i)}} \ : \ \mathbf{j} \in \mathbf{J}_\Omega \right\}, \ \mathbf{J}_\Omega = \{\mathbf{j} = (j_1, j_2) \ : \ j_1, j_2 = 2, \dots, n-3\},$$

$$\boldsymbol{\Phi}_{\Sigma^{(i)}} = \left\{ \phi_{\mathbf{j}}^{\Sigma^{(i)}} \ : \ \mathbf{j} \in \mathbf{J}_\Sigma \right\}, \ \mathbf{J}_\Sigma = \{\mathbf{j} = (j_1, j_2) \ : \ j_1 = 3 - j_2, \dots, n_{j_2} - 4 + j_2; \ j_2 = 0, 1\},$$

and

$$\boldsymbol{\Phi}_{\mathbf{x}^{(i)}} = \left\{ \phi_{\mathbf{j}}^{\mathbf{x}^{(i)}} \ : \ \mathbf{j} \in \mathbf{J}_\chi \right\}, \ \text{with} \ \ \mathbf{J}_\chi = \{\mathbf{j} = (j_1, j_2) : j_1, j_2 = 0, 1, 2; \ j_1 + j_2 \leq 2\}.$$

Thereby, the construction of the single basis functions works analogous to the planar case for the patch interior basis functions $\phi_{\mathbf{j}}^{\Omega^{(i)}}$ and for the edge basis functions $\phi_{\mathbf{j}}^{\Sigma^{(i)}}$, see for instance [34,49], while it has to be slightly adapted for a vertex basis function $\phi_{\mathbf{j}}^{\mathbf{x}^{(i)}}$ by instead of enforcing the C^2 interpolation at the vertex $\mathbf{x}^{(i)}$ with respect to the domain Ω, enforcing it with respect to the tangent plane at $\mathbf{x}^{(i)}$. As in the planar case [34], the patch interior basis functions $\phi_{\mathbf{j}}^{\Omega^{(i)}}$, the edge basis functions $\phi_{\mathbf{j}}^{\Sigma^{(i)}}$ and the vertex basis functions $\phi_{\mathbf{j}}^{\mathbf{x}^{(i)}}$ have small local supports within the patch $\Omega^{(i)}$, in the vicinity of the edge $\Sigma^{(i)}$ and in the vicinity of the vertex $\mathbf{x}^{(i)}$, respectively. Furthermore, the basis functions possess the same local and quasi-local linear independence properties as shown in [49] for the planar case, and which are summarized in the following proposition.

Proposition 2.1. *The C^1 basis functions satisfy the following properties:*

1. *The patch interior and edge basis functions $\boldsymbol{\Phi}_\Omega \cup \boldsymbol{\Phi}_\Sigma$ are locally linearly independent.*
2. *For any vertex $\mathbf{x}^{(i)}, i \in \mathcal{I}_\chi$, and any element Q adjacent to the vertex, the basis functions $\boldsymbol{\Phi}_{\mathbf{x}^{(i)}}$ are linearly independent in Q.*
3. *For any vertex $\mathbf{x}^{(i)}, i \in \mathcal{I}_\chi$, let us define $\Psi_{\mathbf{x}^{(i)}} = \boldsymbol{\Phi} \setminus \boldsymbol{\Phi}_{\mathbf{x}^{(i)}}$. Then, on any element Q adjacent to the vertex it holds that $\operatorname{span}(\boldsymbol{\Phi}_{\mathbf{x}^{(i)}}|_Q) \cap \operatorname{span}(\Psi_{\mathbf{x}^{(i)}}|_Q) = 0$.*

Proof. The three statements of the thesis can be shown analogously to the proofs in [49, Lemma 4.2–4.4] with the one difference that the C^2 interpolation at a vertex $\mathbf{x}^{(i)}$ is performed with respect to the corresponding tangent plane and not with respect to Ω. □

3. Hierarchical C^1 splines on multi-patch surfaces

In this section, we present the construction of hierarchical C^1 splines on multi-patch surfaces leveraging on the results recently presented in [48,49] for the planar two-patch and multi-patch cases, respectively.

3.1. Hierarchical bases of C^1 splines on multi-patch surfaces

We consider a nested sequence of C^1 spline (sub)spaces $\mathbb{A}^0 \subset \mathbb{A}^1 \subset \dots \mathbb{A}^{N-1}$, as defined in Section 2.2, on the multi-patch surface Ω described with an analysis-suitable G^1 parameterization $\mathbf{F}$ as in Section 2.1. The initial space $\mathbb{A}^0$ is defined on the same uniform mesh as the G^1 parameterization $\mathbf{F}$, while any successive space $\mathbb{A}^\ell$, with $\ell > 0$, in the sequence is defined on the meshes obtained by applying dyadic uniform refinement on the elements belonging to the previous level $\ell - 1$. The nestedness of the subspaces $\mathbb{A}^\ell$ defined in this way is a direct consequence of the characterization of the subspaces themselves, see (2) and [49, Proposition 5.1]. The mesh associated to the subspace $\mathbb{A}^\ell$ is denoted by G^ℓ. Each space $\mathbb{A}^\ell$, for $\ell = 0, \dots, N-1$, is then spanned by the basis $\boldsymbol{\Phi}^\ell$ defined as union of patch interior functions $\boldsymbol{\Phi}^\ell_\Omega$, edge functions $\boldsymbol{\Phi}^\ell_\Sigma$, and vertex functions $\boldsymbol{\Phi}^\ell_\chi$ as in (3) with respect to the tensor-product grid G^ℓ.

To introduce the spline hierarchy over the multi-patch surface Ω, we also consider a sequence of closed nested surface domains $\Omega = \Omega^0 \supseteq \Omega^1 \supseteq \dots \supseteq \Omega^{N-1}$. Each subdomain of a certain level ℓ identifies the part of the domain where the corresponding tensor-product grid G^ℓ has to be locally considered. The hierarchical spline basis is defined as follows:

$$\mathcal{H} := \left\{ \phi \in \boldsymbol{\Phi}^\ell \ : \ \operatorname{supp} \phi \subseteq \Omega^\ell \wedge \operatorname{supp} \phi \nsubseteq \Omega^{\ell+1}, \ \ell = 0, \dots, N-1 \right\}.$$

We may exploit the two-scale relation defined by the refinement mask presented in [49] to express any spline $s \in \boldsymbol{\Phi}^\ell$ as linear combination of refined splines in $\boldsymbol{\Phi}^{\ell+1}$

$$s = \sum_{\phi \in \boldsymbol{\Phi}^{\ell+1}} c_\phi^{\ell+1}(s)\, \phi,$$

and define the truncation of s with respect to level $\ell+1$ as

$$\mathrm{trunc}^{\ell+1}(s) := \sum_{\phi\in\Phi^{\ell+1},\,\mathrm{supp}\,\phi\not\subseteq\Omega^{\ell+1}} c_\phi^{\ell+1}(s)\,\phi.$$

The truncated hierarchical spline basis is defined as follows

$$\mathcal{T} := \left\{\mathrm{Trunc}^{\ell+1}(\phi) : \phi\in\Psi^\ell\cap\mathcal{H},\ \ell=0,\dots,N-1\right\},\quad \text{with}\quad \mathrm{Trunc}^{\ell+1}(\phi) := \mathrm{trunc}^{N-1}\left(\dots\left(\mathrm{trunc}^{\ell+1}(\phi)\right)\dots\right)$$

and $\mathrm{Trunc}^N(\phi) = \phi$. In this construction, finer basis functions introduced in the hierarchical basis are removed from the representation of coarser basis functions to reduce the overlap of basis supports at different resolution levels. In the single-patch B-spline setting, truncated hierarchical B-splines (THB-splines) were introduced exploiting standard B-spline refinement schemes and recovering the partition of unity property, see e.g., [47,52,53]. The linear independence of (T)HB-splines is a direct consequence of the local linear independence of B-splines [47]. This property does not hold for the C^1 splines here considered, but the linear independence of (truncated) hierarchical C^1 splines on multi-patch configurations is recovered under the assumption of the following theorem, as proved in [49]. Note that a weaker assumption than local linear independence for hierarchical spline constructions was also previously considered in [54].

Theorem 3.1. *If for every active vertex function of level ℓ, associated to the vertex $\mathbf{x}^{(i)}$, there exists an active element of level ℓ adjacent to the vertex $\mathbf{x}^{(i)}$, both $\mathcal{H}$ and $\mathcal{T}$ are linearly independent.*

This means that if a vertex function of level ℓ is active, there must be an active element of the same level adjacent to the same vertex. This condition can be easily guaranteed by suitable refinement and coarsening algorithms.

3.2. Refinement algorithm on AS G^1 multi-patch surfaces

Let each surface domain Ω^ℓ, for $\ell=1,\dots,N-1$, be defined as union of elements of the grid of level $\ell-1$. The hierarchical mesh $\mathcal{Q}$

$$\mathcal{Q} := \left\{Q\in\mathcal{G}^\ell,\ \ell=0,\dots,N-1\right\},\quad \text{with}\quad \mathcal{G}^\ell := \left\{Q\in G^\ell : Q\subset\Omega^\ell\wedge Q\not\subset\Omega^{\ell+1}\right\},$$

is defined as the collection of surface elements $\mathcal{G}^\ell$ activated at different levels. We say that the hierarchical mesh $\mathcal{Q}$ is admissible of class m if the (T)HB-splines in $\mathcal{T}(\mathcal{Q})$ which take non-zero values over any mesh element $Q\in\mathcal{Q}$ belong to at most m successive levels. This class of hierarchical meshes collects structured graded meshes where the number of (truncated) hierarchical functions acting on a single element does not depend on the number of hierarchical levels.

The refinement algorithm proceeds as follows. Given a set of mesh elements marked for refinement, an additional set of elements of coarser levels will also be refined, to guarantee that on any element of the refined mesh only a *bounded* number of (truncated) hierarchical functions will be non zero. The specific bound to be considered depends on the chosen class of admissibility m: on any active element of the hierarchical mesh constructed with the admissible refinement approach, only hierarchical basis functions introduced at (maximum) m different levels will be active. The considered refinement algorithm for THB-splines has been introduced in [55] to prove the converge of the adaptive isogeometric method. The refinement scheme to address the multi-patch setting was presented in [49], and it extends directly to the surface case.

When C^1 hierarchical spline functions on multi-patch surfaces are considered, the refinement algorithm does not only need to preserve the admissibility of the hierarchical mesh configuration, but also the linear independence of the basis functions. To guarantee this, whenever an element of level ℓ adjacent to a vertex is marked for refinement, every element in its *vertex-patch neighborhood* is also refined. The vertex-patch neighborhood collects all active elements of level ℓ belonging to the same patch as the marked element, and contained in the support of vertex functions associated to the considered vertex. Fig. 1(a–b) show what happens when an element adjacent to a vertex is marked for refinement: the elements of its level contained in its vertex-patch neighborhood are also refined. If the marked element is not adjacent to a vertex instead, no further elements are refined, even if it belongs to the support of a vertex function, see Fig. 1(c–d).

Note that, when the adaptive scheme needs to perform both refinement and coarsening during the simulation, an analogous algorithm to coarsen the multi-patch hierarchical discretization can be considered [50]. The algorithm preserves both the mesh admissibility property, and the linear independence of the hierarchical basis functions.

4. Adaptive method for fourth order partial differential equations

In this section we detail the adaptive approach for the solution of fourth order PDEs on surfaces, based on the hierarchical C^1 spaces of Section 3. We will first present the adaptive method in a general framework, and show examples by applying it to the solution of the bilaplacian problem and to Kirchhoff–Love shells. All the numerical tests are run using the GeoPDEs library [56,57], and the code to reproduce them has been incorporated into the latest version of the library.

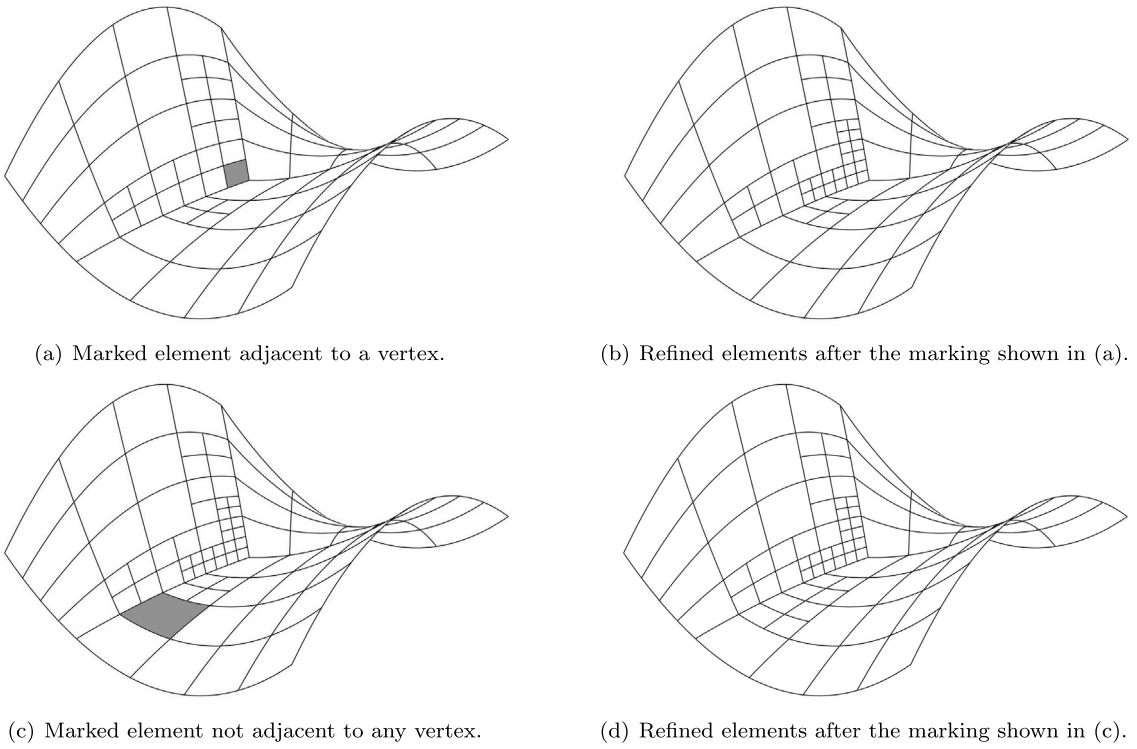

(a) Marked element adjacent to a vertex.

(b) Refined elements after the marking shown in (a).

(c) Marked element not adjacent to any vertex.

(d) Refined elements after the marking shown in (c).

Fig. 1. If an element adjacent to a vertex is marked for refinement, highlighted in dark gray in (a), all the elements in its vertex-patch neighborhood must be also refined (b). If the marked element is not adjacent to any vertex (c), no additional elements need to be refined (d), even if the marked element belongs to the support of vertex basis functions.

4.1. General adaptive framework

The structure of the method follows the widely employed adaptive loop (see, e.g., [41])

$$\text{SOLVE} \longrightarrow \text{ESTIMATE} \longrightarrow \text{MARK} \longrightarrow \text{REFINE}. \tag{4}$$

At each step of the adaptive loop we have a hierarchical mesh on which we define a discrete space V_h of hierarchical C^1 splines of degree p, whose precise definition will depend on the particular problem and the boundary conditions. We solve the problem using a Galerkin method, for which we have to consider the variational formulation generally written as

$$a(u_h, v_h) = F(v_h) \quad \text{for all } v_h \in V_h, \tag{5}$$

with the bilinear functional $a : V_h \times V_h \to \mathbb{R}$ and the linear functional $F : V_h \to \mathbb{R}$. Once the solution is computed, it is necessary to estimate the discretization error to decide which region needs to be refined. We use an a posteriori error estimator based on bubble functions, which follows the original idea from [58], and was already applied for the bilaplacian problem and Kirchhoff–Love shells in IGA [59,60]. Although other estimators are possible, such as the residual error estimator, this one has the advantage that it avoids the computation of third or fourth order derivatives. To compute the estimator, we construct a set of bubble functions of degree $p+1$ and C^1 continuity across elements, with support in one single element, and denote the space they span by B_h. Once we have constructed the space of bubble functions, we compute an estimator of the error $\mathbf{e}_h$ as the solution of the problem

$$a(e_h, b_h) = F(b_h) - a(u_h, b_h) \quad \text{for all } b_h \in B_h.$$

Since the bubble functions are supported in one element, the linear system associated to this problem has a block diagonal structure, with one block per element, and is very easy to parallelize. Then, the estimate of the error on each element $Q \in \mathcal{Q}$ is given by computing the energy norm $\|e_h\|^2_{E(Q)} = a(e_h|_Q, e_h|_Q)$. Once we have computed an estimator for each element, we mark the elements to refine following Dörfler's strategy [61]. Finally, the set of marked elements is passed to the algorithm of Section 3.2 in such a way that some additional elements are marked for refinement to maintain admissibility and linear independence of hierarchical C^1 splines. When the mesh is refined, the discrete space is updated accordingly, and a new step of the algorithm begins.

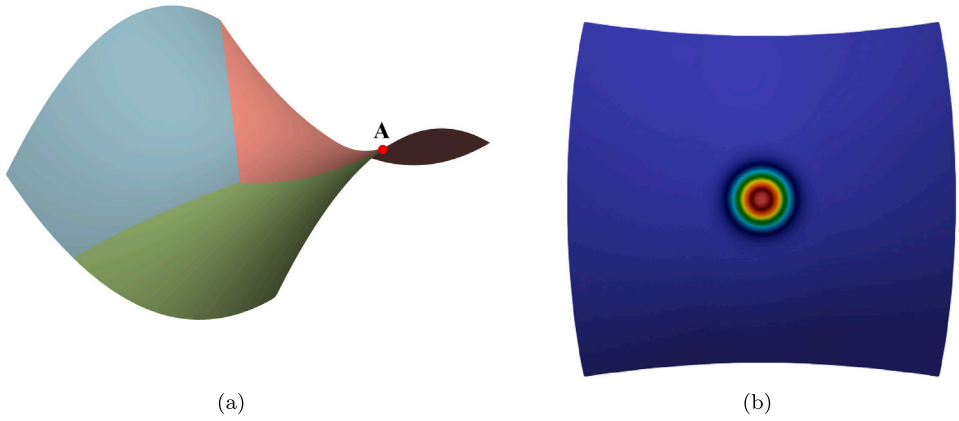

Fig. 2. Domain (a) and exact solution (b) for the bilaplacian problem on a three-patch domain.

4.2. Adaptive method for the bilaplacian problem

We employ the adaptive framework explained above to solve the bilaplacian problem

$$\begin{cases} \Delta^2 u = f & \text{in } \Omega, \\ u = g_1 & \text{on } \partial\Omega, \\ \dfrac{\partial u}{\partial n} = g_2 & \text{on } \partial\Omega. \end{cases}$$

Starting from the discrete space $\mathbb{W}_h := \text{span}\{\mathcal{H}\}$, given by hierarchical C^1 splines of degree p, we first construct a function $u_{b,h} \in \mathbb{W}_h$ satisfying the boundary conditions, which are imposed strongly by a projection onto the space generated by boundary functions. At each step, the problem is to find $u_h \in V_h := \mathbb{W}_h \cap H_0^2(\Omega)$ such that it solves a variational formulation as in (5), with

$$a(u_h, v_h) = \int_\Omega \Delta u_h \Delta v_h, \qquad F(v_h) = \int_\Omega f v_h - \int_\Omega \Delta u_{b,h} \Delta v_h.$$

For the computation of the estimator, the space of bubble functions B_h is taken as C^1 splines of degree $p+1$ with support on one single element, and with zero value and derivative on the boundary.

In the following two examples we apply the adaptive isogeometric method with truncated hierarchical C^1 splines of degree $p = 3, 4, 5$ and regularity $r = p - 2$ in the interior of the patches. For refinement we use admissible meshes with admissibility class $m = 3$, and when deciding the elements to mark we choose Dörfler's parameter equal to 0.75. We compare the results with those obtained with the same spline spaces but refining uniformly.

4.2.1. Peak on a three-patch hyperboloid

As first test, we solve the bilaplacian problem on a three-patch hyperboloid described by dividing the square $(-0.5, 0.5)^2$ in three patches at point $(0.05, -0.1)$, and then mapping it with the parameterization $(x, y, x^2 - y^2)$ as shown in Fig. 2(a). The right-hand side and boundary conditions are chosen to have the exact solution represented in Fig. 2(b), and given by

$$u(x, y, z) = e^{-200\,(x^2+y^2+z^2)}, \qquad (x, y, z) \in \Omega.$$

This solution is smooth, but it clearly has a peak at $(0, 0, 0)$. We tested the adaptive isogeometric method starting at the first iteration from a coarse 4×4 mesh in each patch. The obtained meshes show that the refinement is localized around $(0, 0, 0)$, see Fig. 3(a)–(c). The convergence plot of the error in H^2 seminorm, shown in Fig. 3(d), indicates that the use of the C^1 multi-patch space did not spoil the optimal convergence rates, leading to an evident advantage over the uniform refinement in terms of degrees of freedom.

4.2.2. Singular solution on a five-patch domain

As second example, we solve the bilaplacian problem on the five-patch geometry in Fig. 4(a), which is created by removing a patch from the six-patch geometry approximating the sphere, already employed in the tests of the C^1 space in [31]. We apply homogeneous boundary conditions, and a uniform right-hand side $f = 1$. The reference solution, obtained by solving the problem on a very fine uniform mesh, is shown in Fig. 4(b). The solution is known to have singularities at the four corners of the boundary (see Fig. 4(c)). We applied the adaptive isogeometric method starting with a coarse 2×2 mesh in each patch. As expected, the refinement is localized around the singularities at the corners of the boundary, see Fig. 5(a)–(c). The plot in Fig. 5(d) reports the behavior of the estimator (since we do not have the exact solution available), which has optimal convergence like in the previous example, while uniform refinement leads to suboptimal convergence due to the singularities.

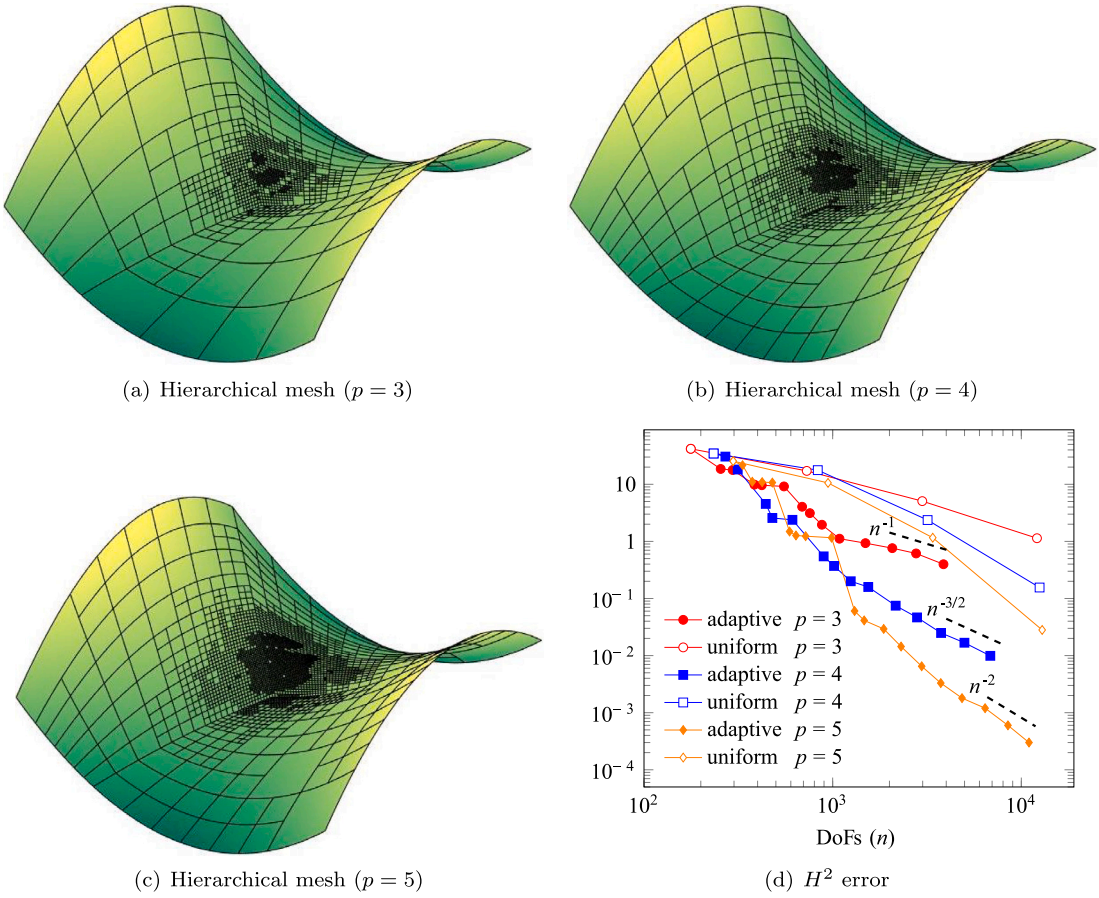

(a) Hierarchical mesh ($p = 3$) (b) Hierarchical mesh ($p = 4$)

(c) Hierarchical mesh ($p = 5$) (d) H^2 error

Fig. 3. Results for bilaplacian on the hyperboloid: obtained hierarchical meshes (a)–(c) and convergence of the error in H^2 seminorm (d).

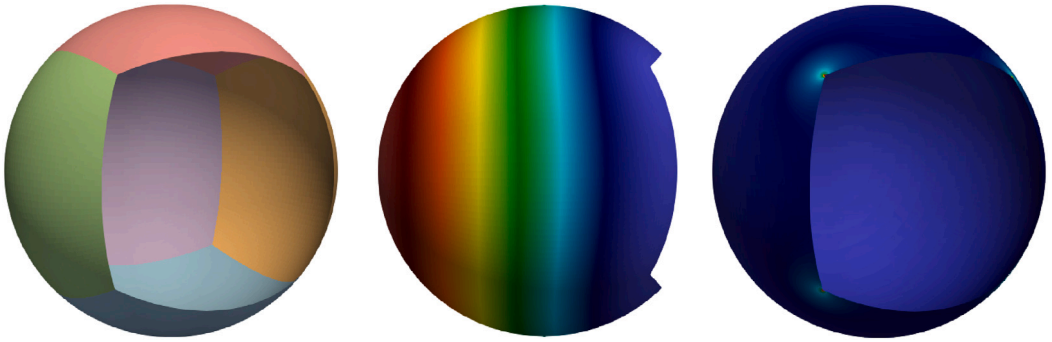

(a) (b) (c)

Fig. 4. Bilaplacian problem on a five-patch domain: domain (a), solution (b) and Laplacian of the solution (c).

4.3. Adaptive method for Kirchhoff–Love shells

As a second problem to apply the adaptive method with C^1 hierarchical splines we consider Kirchhoff–Love shells. With respect to the Reissner–Mindlin formulation, which uses as unknowns both the displacement and the rotation, the Kirchhoff–Love formulation only uses the displacement, reducing the number of degrees of freedom per node. The Kirchhoff–Love shell formulation is a fourth order PDE, which makes it well suited for its solution with IGA. Ensuring global C^1 continuity of the discrete functions in the multipatch setting allows to use a direct formulation, without introducing additional gluing terms at the interfaces between patches.

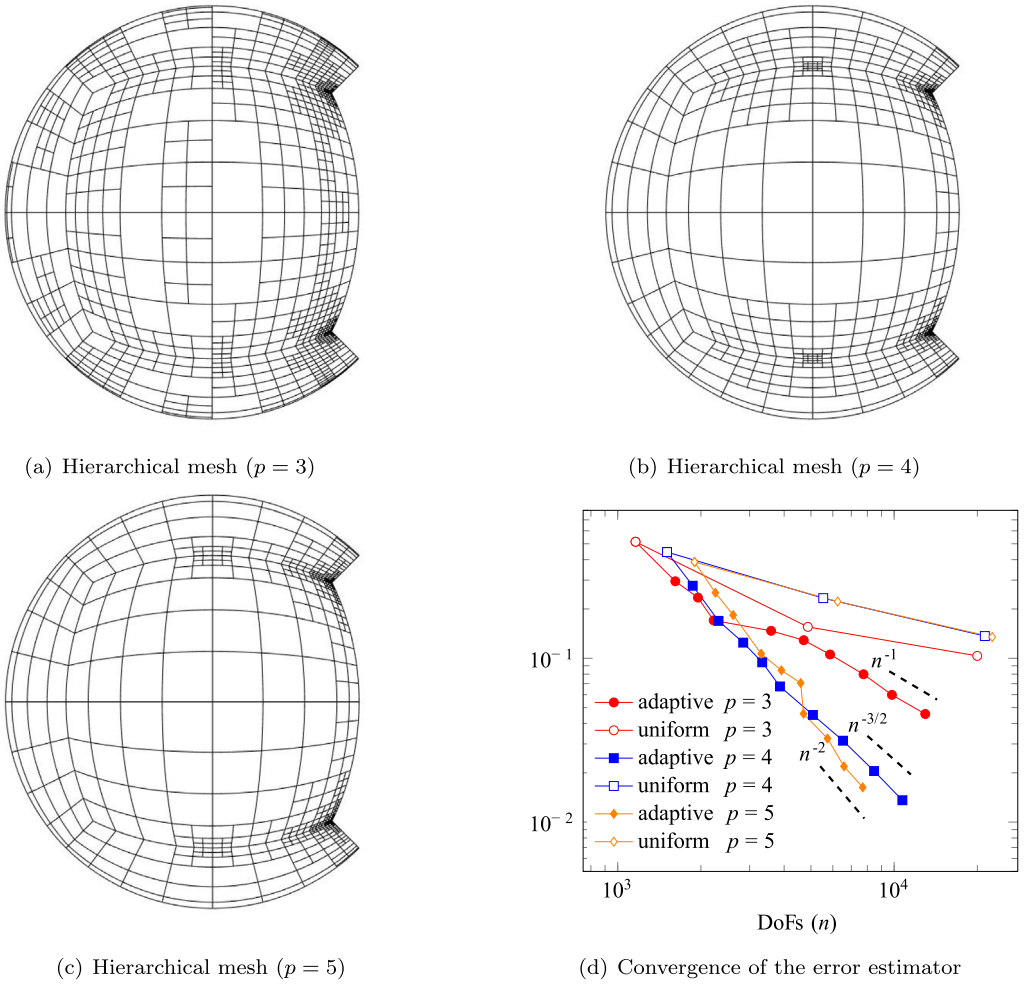

(a) Hierarchical mesh ($p = 3$) (b) Hierarchical mesh ($p = 4$)

(c) Hierarchical mesh ($p = 5$) (d) Convergence of the error estimator

Fig. 5. Bilaplacian on a five-patch domain: obtained hierarchical meshes (a)–(c) and convergence of the estimator (d).

We will apply zero displacement boundary conditions on Γ_{D_1} strongly, and zero rotation boundary conditions are applied on Γ_{D_2} in a weak sense using Nitsche's method following [62]. We note that the intersection of Γ_{D_1} and Γ_{D_2} may not be empty. The discrete variational formulation of the problem is given in the same form as (5), with the bilinear functional $a(\cdot,\cdot)$ and the linear functional $F(\cdot)$ respectively defined as

$$
\begin{aligned}
a(\mathbf{u}_h, \mathbf{v}_h) &= \int_\Omega \boldsymbol{\varepsilon}(\mathbf{u}_h) : \boldsymbol{n}(\mathbf{v}_h)\,\mathrm{d}\Omega + \int_\Omega \boldsymbol{\kappa}(\mathbf{u}_h) : \boldsymbol{m}(\mathbf{v}_h)\,\mathrm{d}\Omega \\
&+ \int_{\Gamma_{D_2}} \frac{C_{\text{pen}}}{h}\,\theta_n(\mathbf{u}_h)\,\theta_n(\mathbf{v}_h)\,\mathrm{d}\Gamma - \int_{\Gamma_{D_2}} \boldsymbol{\kappa}_{nn}(\mathbf{u}_h)\theta_n(\mathbf{v}_h)\,\mathrm{d}\Gamma - \int_{\Gamma_{D_2}} \boldsymbol{\kappa}_{nn}(\mathbf{v}_h)\,\theta_n(\mathbf{u}_h)\,\mathrm{d}\Gamma, \\
F(\mathbf{v}_h) &= \int_\Omega \mathbf{v}_h \cdot \mathbf{f}\,\mathrm{d}\Omega,
\end{aligned}
$$

where $\boldsymbol{\varepsilon}$ and $\boldsymbol{\kappa}$ respectively denote the membrane strain tensor and the bending strain tensor, and $\boldsymbol{n}, \boldsymbol{m}$ are their energetically conjugate stress resultants, see [63–65] for the details, while the $\mathbf{f}$ term appearing on the right-hand side is a given body load. For the terms appearing on the boundary, $\boldsymbol{\kappa}_{nn}$ is the bending moment, θ_n is the normal rotation, h is the local mesh size, and C_{pen} is a penalty parameter that we choose equal to 10, see [62] for the details. Note that in this formulation the unknown is the displacement, which is a vector field, and we impose strongly the zero displacement boundary condition, for which the discrete space is given by

$$
V_h = \{\mathbf{v}_h \in (\mathbb{W}_h)^3 : \mathbf{v}_h = \mathbf{0} \text{ on } \Gamma_{D_1}\}.
$$

We assume for simplicity that on Γ_{D_1} the three components of the displacement are set to zero, but more general problems, for which only some of the displacement components are enforced, can also be considered. The vector valued bubble functions for the error estimator are defined analogously as for the bilaplacian problem, but considering one function for each vector component.

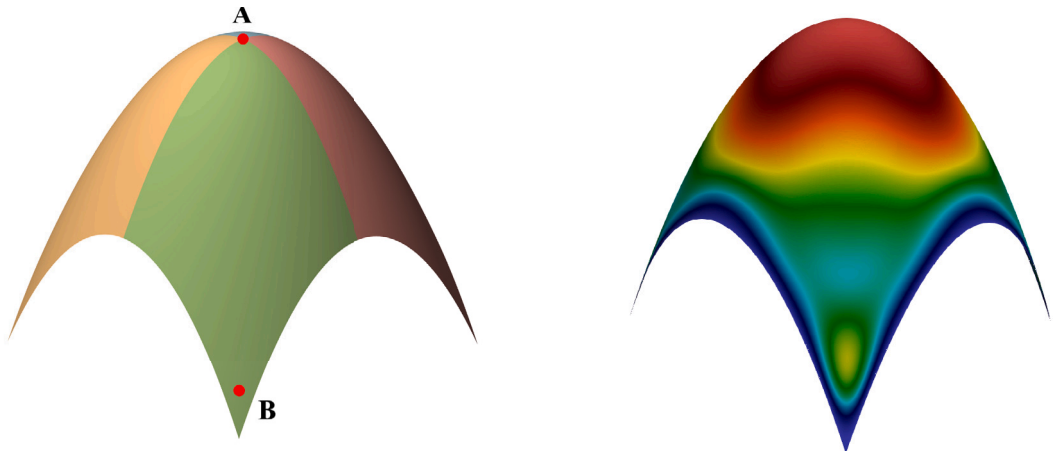

(a) Parameterization of the paraboloid. (b) Magnitude of the displacement.

Fig. 6. Paraboloid Kirchhoff–Love shell: geometry configuration and displacement magnitude.

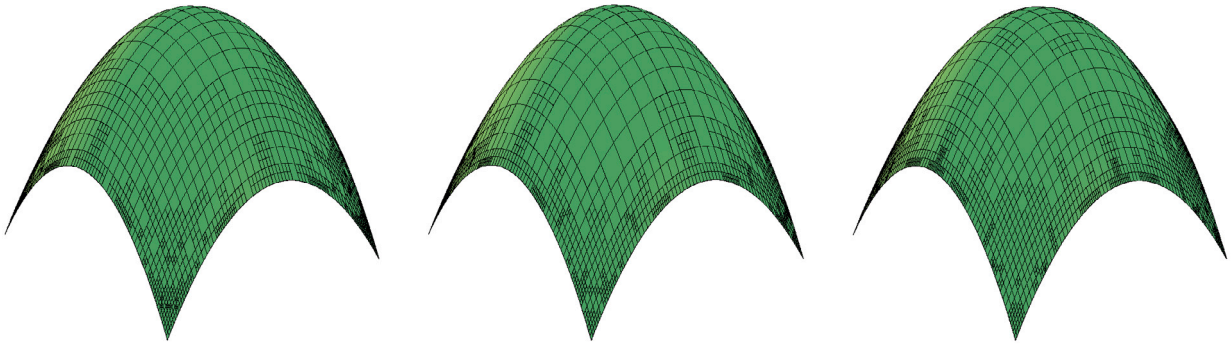

(a) Degree $p = 3$ (2128 elements). (b) Degree $p = 4$ (1804 elements). (c) Degree $p = 5$ (2224 elements).

Fig. 7. Paraboloid Kirchhoff–Love shell. Adaptive meshes at the last step.

In the following two examples we apply the adaptive isogeometric method with truncated hierarchical C^1 splines of degree $p = 3, 4, 5$ and regularity $r = p - 2$ in the interior of the patches. For refinement we use admissible meshes with admissibility class $m = 3$, while Dörfler's parameter is set to 0.8. We compare the results with those obtained with the same spline spaces but refining uniformly.

4.3.1. Paraboloid shell with simply supported boundary

As a first test for Kirchhoff–Love shells we consider a paraboloid geometry with simply supported boundary conditions on the whole boundary. The geometry is built by dividing the square $(-1, 1)^2$ in four patches of equal size, which are then mapped using the parameterization $(x, y, 1 - x^2 - y^2)$, which yields an analysis-suitable geometry shown in Fig. 6(a). The geometric and material properties of the shell considered for the simulation are the thickness $t = 0.01$ [m], Young's modulus $E = 2{\times}10^{11}$ [N/m^2] and Poisson ratio $\nu = 0.3$ [–]. The shell is subject to a uniform vertical load of magnitude 80000 [N/m^2], and we impose zero displacement in all directions for the whole boundary, i.e., $\Gamma_{D_1} = \partial\Omega$ and $\Gamma_{D_2} = \emptyset$. The magnitude of the displacement, computed in a fine mesh for degree 5, is shown in Fig. 6(b).

Starting from a uniform mesh with 4×4 elements per patch, we run adaptive simulations until a maximum number of 15000 degrees of freedom is reached. The final meshes obtained for each degree are shown in Fig. 7. We see that in all cases the domain is more refined towards the boundary, and in particular close to the corners, since it is the region where the stress is higher.

Since the exact solution is not known, to analyze the accuracy of the solution we compare in Fig. 8(a) the convergence of the estimator for adaptive and uniform refinement. We see that the convergence rate is optimal in both cases, because the solution is regular, but adaptive refinement gets lower values of the error with respect to the number of degrees of freedom. We also compare in Fig. 8(b) the behavior during refinement of the energy norm, given by $\frac{1}{2}a(\mathbf{u}_h, \mathbf{u}_h)$ (or in matrix form, $\frac{1}{2}\mathbf{u}^\top K\mathbf{u}$), for adaptive and uniform refinement. We observe that the adaptive case converges much faster in terms of the number of degrees of freedom, and the accuracy is increased for higher degree, as expected. We also analyze the result of vertical displacement at the points $\mathbf{A} = (0, 0, 1)$ and

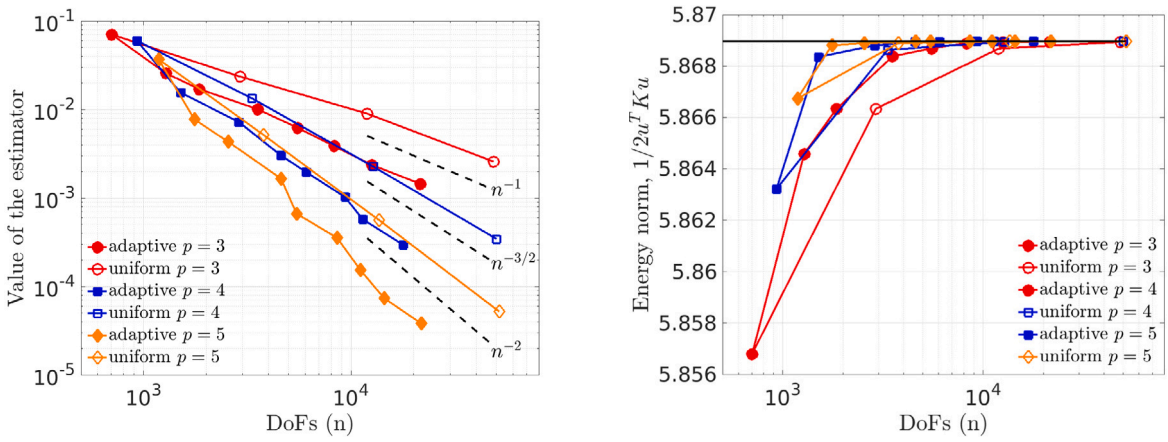

(a) Convergence of the estimator. (b) Value of the energy.

Fig. 8. Paraboloid Kirchhoff–Love shell. Convergence of the estimator and value of the energy.

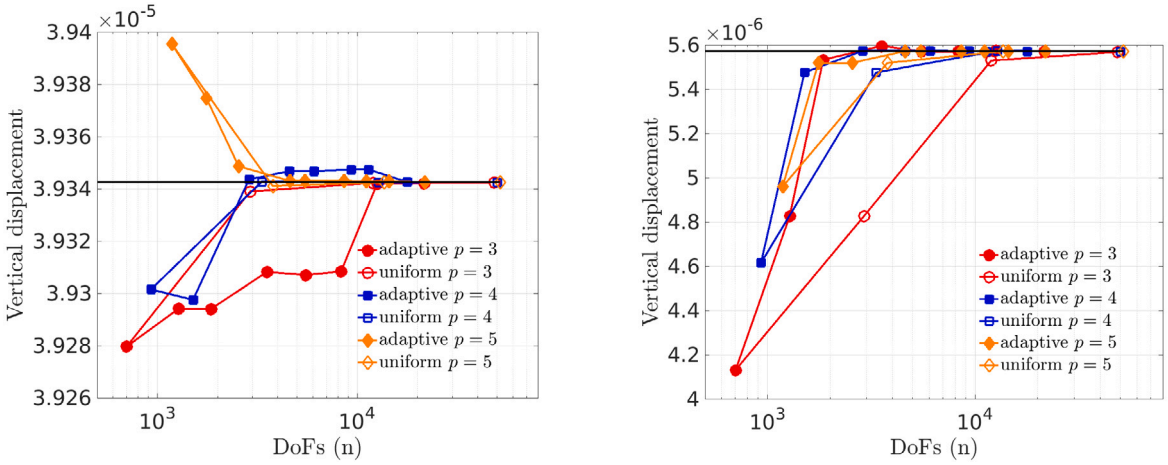

(a) Vertical displacement of point **A**. (b) Vertical displacement of point **B**.

Fig. 9. Paraboloid Kirchhoff–Love shell. Vertical displacement for points **A** and **B**.

B = (0.93, 0.93, −0.7298), the first one corresponding to the tip of the paraboloid, and the second one closer to a vertex, see Fig. 6(a). The results, that we plot in Fig. 9, show in general better behavior of the uniform case for point **A**, and much better behavior of the adaptive case for point **B**. This is expected because, as we said above, the adaptive algorithm concentrates the refinement close to the corners, where point **B** is. To obtain better results for point **A**, a goal-oriented error estimator should be used, but this goes beyond the scope of this work.

4.3.2. Partly clamped hyperboloid shell

As second test we consider a hyperboloid shell, with the same geometry already used in Section 4.2.1, in a test that was already used as a benchmark for finite elements [66]. The same test has been used for the analysis of multipatch IGA methods, without adaptivity, in [2,36,38]. The material parameters used for the simulation are the same as for the paraboloid shell, namely, thickness $t = 0.01$ [m], Young's modulus $E = 2 \times 10^{11}$ [N/m^2] and Poisson ratio $\nu = 0.3$ [–]. We apply a uniform vertical load of magnitude $8000t$ [N/m^2], and we impose zero displacement and zero rotation at the boundary $\Gamma_{D_1} = \Gamma_{D_2}$, which is given by the set of points (x, y, z) such that $x = -0.5$. We show in Fig. 10(a) the magnitude of the displacement for a reference solution, computed in a single patch domain for a very fine uniform mesh of 150 × 150 elements and degree $p = 5$, for approximately 72000 degrees of freedom.

Starting again from a uniform mesh made of 4 × 4 elements on each patch, we run the adaptive simulation until nine levels of refinement are reached. We show in Figs. 10(b)–10(d) the meshes obtained for the different degrees. In this case, the adaptive algorithm concentrates the refinement at the two corners separating the clamped boundary and the free boundary, as it is the region where the maximum stress appears.

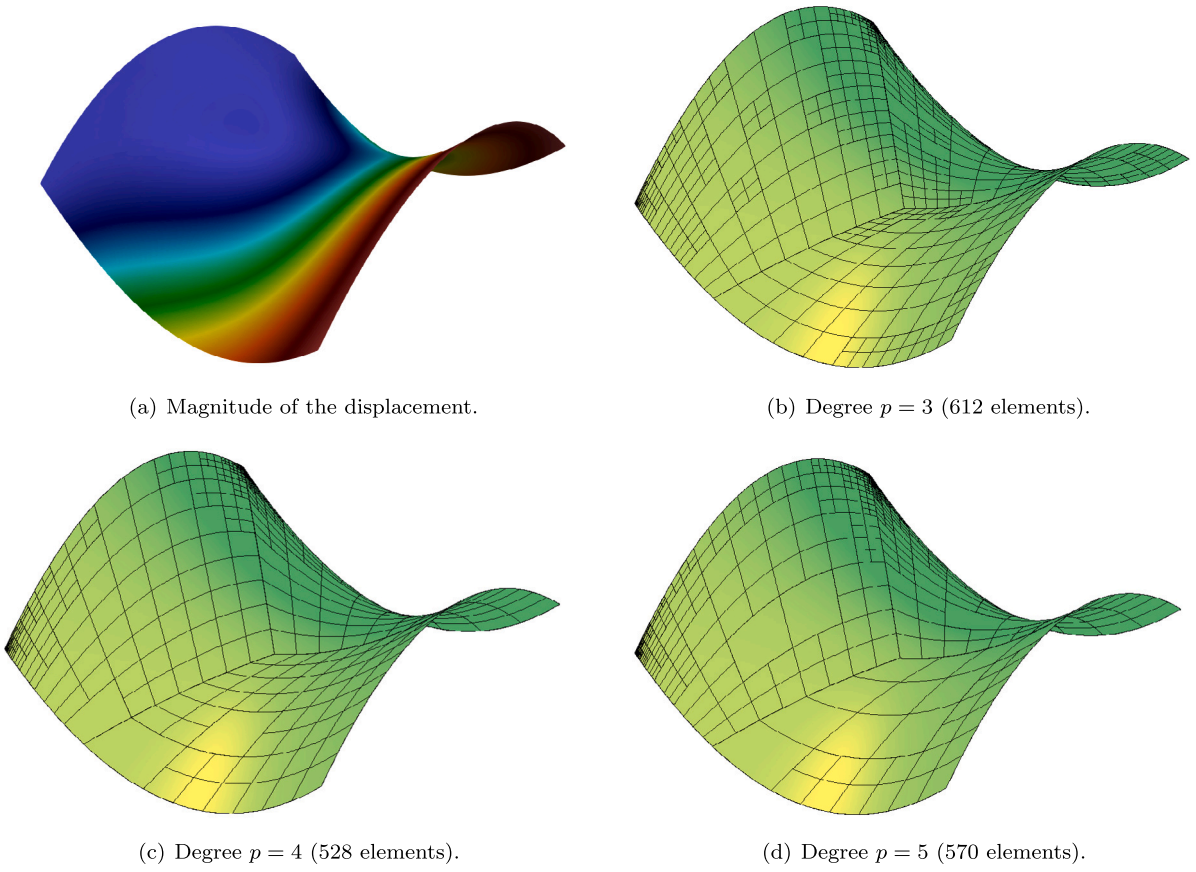

(a) Magnitude of the displacement.

(b) Degree $p = 3$ (612 elements).

(c) Degree $p = 4$ (528 elements).

(d) Degree $p = 5$ (570 elements).

Fig. 10. Hyperboloid Kirchhoff–Love shell. Reference solution, and adaptive meshes at the last step.

To study the accuracy of the adaptive method, we compare in Fig. 11(a) the results of the energy norm for uniform and adaptive refinement, and their convergence towards the reference solution mentioned above, obtained in a very fine mesh for a single patch domain. The adaptive method shows a better behavior compared to the uniform refinement, and the same accuracy is obtained with one order less of degrees of freedom. Moreover, we also analyze the vertical displacement at the point $\mathbf{A} = (0.5, 0, -0.25)$, located at the middle point of the edge opposite to the clamped side, see Fig. 2(a). The results, displayed in Fig. 11(b), show a similar behavior as for the energy, with higher accuracy of the adaptive method compared to uniform refinement. In contrast to the example of the paraboloid shell, this is true even if the point is far away from the highly refined region.

It is known that a displacement-only discretization as we are using causes membrane locking, and the results in Fig. 11 confirm that our adaptive method is not free from locking, although local refinement can mitigate its effects. There exist other shell elements in the finite element literature, and in particular the Mixed Interpolation of Tensorial Components (MITC) elements [66] or their enriched versions [67], that overcome locking. This comes at the cost of a higher number of degrees of freedom per element. Moreover, the use of isogeometric methods also allows a better representation of curved geometries, which leads to better accuracy with few elements, but it is important to note that the MITC element has been recently generalized to the isogeometric setting [68]. Finally, the analysis of methods to remove membrane locking is an active research topic in IGA (see [69,70] and references therein), and the feasibility of extending these methods to the hierarchical multipatch C^1-setting should be analyzed.

A note about the computational time. To better understand the performance of the method, we present convergence results for the computed energy and for the vertical displacement at point $\mathbf{A}$ with respect to the computational time, instead of the number of degrees of freedom as in Fig. 11. When performing uniform refinement the computational time takes into account the evaluation of the basis functions at quadrature points, the assembly of the matrix and the right-hand side, and the solution of the linear system. For adaptive refinement we also take into account the computation of the a posteriori error estimator, and the refinement of the mesh at each iteration. All the simulations are run on a workstation with system specifications: 12th Gen Intel® Core™ i5-12400 × 12, 16 Gb DDR4 memory. The software environment is Matlab 2023b running on Ubuntu 22.04.4, and all simulations are performed using a single thread. The code is run ten times for each case, and we consider the average of the computational times.

The obtained results are presented in Fig. 12, where for better visualization we plot in logarithmic scale the difference in absolute value with respect to the reference solution. We remark that the computational time for uniform refinement refers to the solution

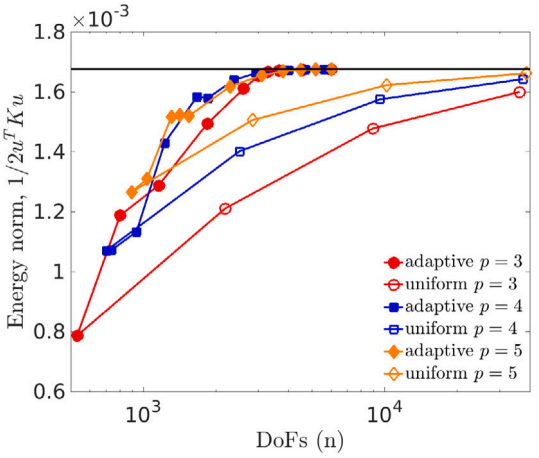

(a) Value of the energy.

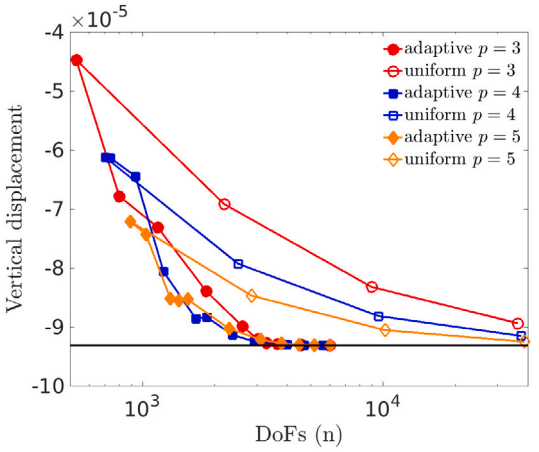

(b) Vertical displacement of point $\mathbf{A} = (0.5, 0, -0.25)$.

Fig. 11. Clamped hyperboloid Kirchhoff–Love shell. Convergence of the energy, and of the vertical displacement at point $(0.5, 0, -0.25)$.

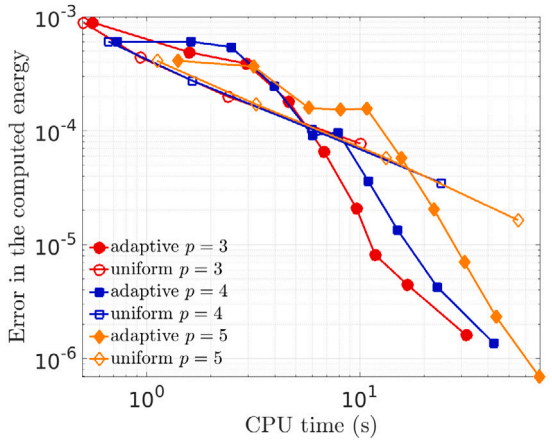

(a) Value of the energy.

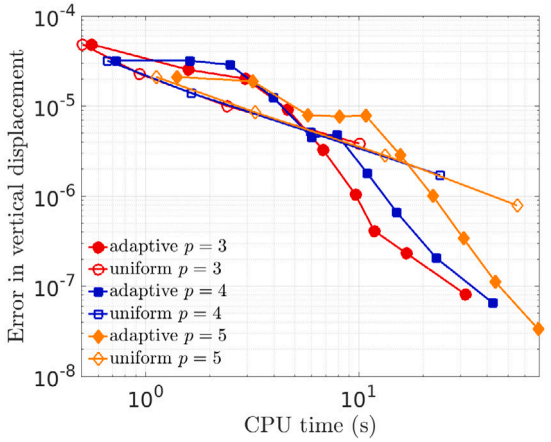

(b) Vertical displacement of point $\mathbf{A} = (0.5, 0, -0.25)$.

Fig. 12. Clamped hyperboloid Kirchhoff–Love shell. Convergence of the energy, and vertical displacement at point $(0.5, 0, -0.25)$.

for a single mesh, while the time for adaptive refinement takes into account all the iterations of the adaptive process, starting from the coarsest mesh. We observe that, when the meshes are coarse, the simulation with uniform meshes is more accurate than the adaptive one, independently of the degree, and this is because the cost of the estimator and the adaptive refinement is relatively large with respect to the solution of the linear system. As soon as the mesh gets finer, the adaptive method performs better than the uniform one, because the local refinement gives much smaller linear systems, and therefore lower computational cost. It is also worth to note that, in our implementation, increasing the degree does not pay off for any of the methods, but this probably depends strongly on the implementation. These results suggest that computing on a coarse uniform mesh performs well when low accuracy is acceptable, but if very accurate results are needed, the adaptive method performs better. Obviously, if the need for local refinement is identified a priori, based on engineering expertise, a hierarchical mesh can be used as the starting point to run the adaptive procedure, in practice saving the computational effort for the first iterations.

Finally, it is important to remark that the presented results can give a qualitative idea of the performance of each method, but the conclusions should be taken with care. Indeed, the code used for computational comparison is not efficient for any of the methods, and all the simulations were run on a single core with a single thread. A more rigorous comparison of the methods should be done using a more efficient implementation, preferably in a compiled language, but this is beyond the scope of the present work.

5. Conclusions

An adaptive isogeometric method for solving fourth order PDEs on multi-patch surfaces and shells was presented. In particular, we extended previous results recently obtained in the planar setting to the case of analysis-suitable G^1 multi-patch surfaces and the

Kirchhoff–Love shell problem. The numerical experiments validate the behavior of the adaptive scheme based on C^1 hierarchical spline on a selection of different test cases. Thanks to the local refinement capabilities of the proposed adaptive method, optimal convergence rates are obtained even when singular solutions of different nature are considered.

CRediT authorship contribution statement

Cesare Bracco: Writing – review & editing, Writing – original draft, Visualization, Software, Investigation, Data curation, Conceptualization. **Andrea Farahat:** Software, Methodology, Investigation, Data curation. **Carlotta Giannelli:** Writing – review & editing, Writing – original draft, Project administration, Methodology, Investigation, Funding acquisition, Formal analysis, Conceptualization. **Mario Kapl:** Writing – review & editing, Writing – original draft, Project administration, Methodology, Investigation, Funding acquisition, Formal analysis, Conceptualization. **Rafael Vázquez:** Writing – review & editing, Writing – original draft, Visualization, Software, Investigation, Data curation, Conceptualization.

Declaration of competing interest

The authors declare the following financial interests/personal relationships which may be considered as potential competing interests: Andrea Farahat reports financial support was provided by Austrian Science Fund. Mario Kapl reports financial support was provided by Austrian Science Fund. Carlotta Giannelli reports financial support was provided by Francesco Severi National Institute of Higher Mathematics. Cesare Bracco reports financial support was provided by Francesco Severi National Institute of Higher Mathematics. Carlotta Giannelli reports was provided by European Union - NextGeneratonEU. Cesare Bracco reports was provided by European Union - NextGeneratonEU. Carlotta Giannelli reports was provided by Italian Ministry of University and Research. Cesare Bracco reports financial support was provided by Italian Ministry of University and Research. If there are other authors, they declare that they have no known competing financial interests or personal relationships that could have appeared to influence the work reported in this paper.

Data availability

The input data considered in the examples are specified in the paper.

Acknowledgments

The authors would like to thank Giuliano Guarino for sharing his implementation of Nitsche's method for shells. Andrea Farahat and Mario Kapl have been supported by the Austrian Science Fund (FWF) through the project P 33023-N. These supports are gratefully acknowledged. Cesare Bracco, and Carlotta Giannelli are members of INdAM research group GNCS, Italy. The INdAM-GNCS support through the SUNRISE Project and Progetti di Ricerca GNCS 2023 " Tecniche spline innovative per metodi di approssimazione e isogeometrici adattivi" is gratefully acknowledged. In addition, Cesare Bracco and Carlotta Giannelli acknowledge the contribution of the National Recovery and Resilience Plan, Mission 4 Component 2 – Investment 1.4 – National Center for HPC, Big Data and Quantum Computing – funded by the European Union – NextGenerationEU – CUP (B83C22002830001). The partial support of the Italian Ministry of University and Research (MUR) through the PRIN projects COSMIC (No. 2022A79M75) and NOTES (No. P2022NC97R), funded by the European Union - NextGenerationEU, is also acknowledged.

References

[1] J.A. Cottrell, T.J.R. Hughes, Y. Bazilevs, Isogeometric Analysis: Toward Integration of CAD and FEA, John Wiley & Sons, Chichester, England, 2009.
[2] H.M. Verhelst, P. Weinmüller, A. Mantzaflaris, T. Takacs, D. Toshniwal, A comparison of smooth basis constructions for isogeometric analysis, Comput. Methods Appl. Mech. Engrg. 419 (2024) 116659.
[3] L. Coradello, G. Loli, A. Buffa, A projected super-penalty method for the C^1-coupling of multi-patch isogeometric Kirchhoff plates, Comput. Mech. 67 (4) (2021) 1133–1153.
[4] A.J. Herrema, E.L. Johnson, D. Proserpio, M.C.H. Wu, J. Kiendl, M.-C. Hsu, Penalty coupling of non-matching isogeometric Kirchhoff–Love shell patches with application to composite wind turbine blades, Comput. Methods Appl. Mech. Engrg. 346 (2019) 810–840.
[5] Y. Guo, M. Ruess, Nitsche's method for a coupling of isogeometric thin shells and blended shell structures, Comp. Methods Appl. Mech. Engrg. 284 (2015) 881–905.
[6] V.P. Nguyen, P. Kerfriden, M. Brino, S. Bordas, E. Bonisoli, Nitsche's method for two and three dimensional NURBS patch coupling, Comput. Mech. 53 (6) (2014) 1163–1182.
[7] R. Bouclier, J.C. Passieux, M. Salaün, Development of a new, more regular, mortar method for the coupling of NURBS subdomains within a NURBS patch: Application to a non-intrusive local enrichment of NURBS patches, Comput. Methods Appl. Mech. Engrg. 316 (2017) 123–150.
[8] T. Horger, A. Reali, B. Wohlmuth, L. Wunderlich, A hybrid isogeometric approach on multi-patches with applications to Kirchhoff plates and eigenvalue problems, Comput. Methods Appl. Mech. Engrg. 348 (2019) 396–408.
[9] A. Seiler, B. Jüttler, Approximately C^1-smooth isogeometric functions on two-patch domains, in: Isogeometric Analysis and Applications 2018, in: Lect. Notes Comput. Sci. Eng., vol. 133, Springer, 2021, pp. 157–175.
[10] T. Takacs, D. Toshniwal, Almost-C^1 splines: Biquadratic splines on unstructured quadrilateral meshes and their application to fourth order problems, Comput. Methods Appl. Mech. Engrg. 403 (2023) 115640.
[11] P. Weinmüller, T. Takacs, An approximate C^1 multi-patch space for isogeometric analysis with a comparison to Nitsche's method, Comput. Methods Appl. Mech. Engrg. 401 (2022) 115592.

[12] P. Weinmüller, T. Takacs, Construction of approximate C^1 bases for isogeometric analysis on two-patch domains, Comput. Methods Appl. Mech. Engrg. 385 (2021) 114017.
[13] T. Nguyen, J. Peters, Refinable C^1 spline elements for irregular quad layout, Comput. Aided Geom. Design 43 (2016) 123–130.
[14] D. Toshniwal, H. Speleers, T.J.R. Hughes, Smooth cubic spline spaces on unstructured quadrilateral meshes with particular emphasis on extraordinary points: Geometric design and isogeometric analysis considerations, Comput. Methods Appl. Mech. Engrg. 327 (2017) 411–458.
[15] X. Wei, X. Li, K. Qian, T.J.R. Hughes, Y.J. Zhang, H. Casquero, Analysis-suitable unstructured T-splines: Multiple extraordinary points per face, Comput. Methods Appl. Mech. Engrg. 391 (2022) 114494.
[16] U. Reif, A refinable space of smooth spline surfaces of arbitrary topological genus, J. Approx. Theory 90 (2) (1997) 174–199.
[17] F. Cirak, M. Ortiz, P. Schröder, Subdivision surfaces: a new paradigm for thin-shell finite-element analysis, Internat. J. Numer. Methods Engrg. 47 (12) (2000) 2039–2072.
[18] A. Riffnaller-Schiefer, U.H. Augsdörfer, D. Fellner, Isogeometric shell analysis with NURBS compatible subdivision surfaces, Appl. Math. Comput. 272 (2016) 139–147.
[19] Q. Zhang, M. Sabin, F. Cirak, Subdivision surfaces with isogeometric analysis adapted refinement weights, Comput.-Aided Des. 102 (2018) 104–114.
[20] K. Karčiauskas, J. Peters, Refinable G^1 functions on G^1 free-form surfaces, Comput. Aided Geom. Design 54 (2017) 61–73.
[21] K. Karčiauskas, J. Peters, Refinable bi-quartics for design and analysis, Comput.-Aided Des. 102 (2018) 204–214.
[22] T. Nguyen, K. Karčiauskas, J. Peters, C^1 finite elements on non-tensor-product 2d and 3d manifolds, Appl. Math. Comput. 272 (2016) 148–158.
[23] Z. Wen, M.S. Faruque, X. Li, X. Wei, H. Casquero, Isogeometric analysis using G-spline surfaces with arbitrary unstructured quadrilateral layout, Comput. Methods Appl. Mech. Engrg. 408 (2023) 115965.
[24] M. Bercovier, T. Matskewich, Smooth Bézier Surfaces over Unstructured Quadrilateral Meshes, Lecture Notes of the Unione Matematica Italiana, vol. 22, Springer, 2017.
[25] M. Kapl, F. Buchegger, M. Bercovier, B. Jüttler, Isogeometric analysis with geometrically continuous functions on planar multi-patch geometries, Comput. Methods Appl. Mech. Engrg. 316 (2017) 209–234.
[26] M. Kapl, G. Sangalli, T. Takacs, A family of C^1 quadrilateral finite elements, Adv. Comput. Math. 47 (2021) 82.
[27] A. Blidia, B. Mourrain, G. Xu, Geometrically smooth spline bases for data fitting and simulation, Comput. Aided Geom. Design 78 (2020) 101814.
[28] C. Chan, C. Anitescu, T. Rabczuk, Strong multipatch C^1-coupling for isogeometric analysis on 2D and 3D domains, Comput. Methods Appl. Mech. Engrg. 357 (2019) 112599.
[29] B. Mourrain, R. Vidunas, N. Villamizar, Dimension and bases for geometrically continuous splines on surfaces of arbitrary topology, Comput. Aided Geom. Design 45 (2016) 108–133.
[30] A. Collin, G. Sangalli, T. Takacs, Analysis-suitable G^1 multi-patch parametrizations for C^1 isogeometric spaces, Comput. Aided Geom. Design 47 (2016) 93–113.
[31] A. Farahat, B. Jüttler, M. Kapl, T. Takacs, Isogeometric analysis with C^1-smooth functions over multi-patch surfaces, Comput. Methods Appl. Mech. Engrg. 403 (2023) 115706.
[32] A. Farahat, M. Kapl, A. Kosmač, V. Vitrih, A locally based construction of analysis-suitable G^1 multi-patch spline surfaces, Comput. Math. Appl. 168 (2024) 46–57.
[33] M. Kapl, G. Sangalli, T. Takacs, Construction of analysis-suitable G^1 planar multi-patch parameterizations, Comput.-Aided Des. 97 (2018) 41–55.
[34] M. Kapl, G. Sangalli, T. Takacs, An isogeometric C^1 subspace on unstructured multi-patch planar domains, Comput. Aided Geom. Design 69 (2019) 55–75.
[35] M. Kapl, G. Sangalli, T. Takacs, Isogeometric analysis with C^1 functions on unstructured quadrilateral meshes, SMAI J. Comput. Math. 5 (2019) 67–86.
[36] A. Farahat, H.M. Verhelst, J. Kiendl, M. Kapl, Isogeometric analysis for multi-patch structured Kirchhoff-Love shells, Comput. Methods Appl. Mech. Engrg. 411 (2023) 116060.
[37] J. Arf, M. Reichle, S. Klinkel, B. Simeon, Scaled boundary isogeometric analysis with C^1 coupling for Kirchhoff plate theory, Comput. Methods Appl. Mech. Engrg. 415 (2023) 116198.
[38] M.F.M. Reichle, J. Arf, B. Simeon, S. Klinkel, Smooth multi-patch scaled boundary isogeometric analysis for Kirchhoff-Love shells, Meccanica 58 (8) (2023) 1693–1716.
[39] R.H. Nochetto, K.G. Siebert, A. Veeser, Theory of adaptive finite element methods: an introduction, in: Multiscale, Nonlinear and Adaptive Approximation, Springer, 2009, pp. 409–542.
[40] R.H. Nochetto, A. Veeser, Primer of adaptive finite element methods, in: Multiscale and Adaptivity: Modeling, Numerics and Applications, in: Lecture Notes in Math., vol. 2040, Springer, Heidelberg, 2012, pp. 125–225.
[41] A. Buffa, G. Gantner, C. Giannelli, D. Praetorius, R. Vázquez, Mathematical foundations of adaptive isogeometric analysis, Arch. Comput. Methods Eng. 29 (2022) 4479–4555.
[42] M.A. Scott, R.N. Simpson, J.A. Evans, S. Lipton, S.P.A. Bordas, T.J.R. Hughes, T.W. Sederberg, Isogeometric boundary element analysis using unstructured T-splines, Comput. Methods Appl. Mech. Engrg. 254 (2013) 197–221.
[43] X. Wei, Y. Zhang, L. Liu, T.J.R. Hughes, Truncated T-splines: fundamentals and methods, Comput. Methods Appl. Mech. Engrg. 316 (2017) 349–372.
[44] X. Wei, Y. Zhang, T.J.R. Hughes, M.A. Scott, Truncated hierarchical catmull-clark subdivision with local refinement, Comput. Methods Appl. Mech. Engrg. 291 (2015) 1–20.
[45] H. Casquero, X. Wei, D. Toshniwal, A. Li, T.J.R. Hughes, J. Kiendl, Y.J. Zhang, Seamless integration of design and Kirchhoff-Love shell analysis using analysis-suitable unstructured T-splines, Comput. Methods Appl. Mech. Engrg. 360 (2020) 112765.
[46] X. Wei, THU-splines: Highly localized refinement on smooth unstructured splines, in: C. Manni, H. Speleers (Eds.), Geometric Challenges in Isogeometric Analysis, Springer International Publishing, Cham, 2022, pp. 305–332.
[47] C. Giannelli, B. Jüttler, H. Speleers, Strongly stable bases for adaptively refined multilevel spline spaces, Adv. Comput. Math. 40 (2014) 459–490.
[48] C. Bracco, C. Giannelli, M. Kapl, R. Vázquez, Isogeometric analysis with C^1 hierarchical functions on planar two-patch geometries, Comput. Math. Appl. 80 (2020) 2538–2562.
[49] C. Bracco, C. Giannelli, M. Kapl, R. Vázquez, Adaptive isogeometric methods with (C^1) (truncated) hierarchical splines on planar multi-patch domains, Math. Models Methods Appl. Sci. 33 (2023) 1829–1874.
[50] C. Bracco, C. Giannelli, A. Reali, M. Torre, R. Vázquez, Adaptive isogeometric phase-field modeling of the cahn-hilliard equation: suitably graded hierarchical refinement and coarsening on multi-patch geometries, Comput. Methods Appl. Mech. Engrg. 417 (2023) 116355.
[51] M. Kapl, G. Sangalli, T. Takacs, Dimension and basis construction for analysis-suitable G^1 two-patch parameterizations, Comput. Aided Geom. Design 52–53 (2017) 75–89.
[52] C. Giannelli, B. Jüttler, H. Speleers, THB–splines: the truncated basis for hierarchical splines, Comput. Aided Geom. Design 29 (2012) 485–498.
[53] C. Giannelli, B. Jüttler, S.K. Kleiss, A. Mantzaflaris, B. Simeon, J. Špeh, THB-splines: An effective mathematical technology for adaptive refinement in geometric design and isogeometric analysis, Comput. Methods Appl. Mech. Engrg. 299 (2016) 337–365.
[54] U. Zore, B. Jüttler, J. Kosinka, On the linear independence of truncated hierarchical generating systems, J. Comput. Appl. Math. 306 (2016) 200–216.
[55] A. Buffa, C. Giannelli, Adaptive isogeometric methods with hierarchical splines: Error estimator and convergence, Math. Models Methods Appl. Sci. 26 (2016) 1–25.
[56] R. Vázquez, A new design for the implementation of isogeometric analysis in Octave and Matlab: GeoPDEs 3.0, Comput. Math. Appl. 72 (2016) 523–554.

[57] E. Garau, R. Vázquez, Algorithms for the implementation of adaptive isogeometric methods using hierarchical B-splines, Appl. Numer. Math. 123 (2018) 58–87.
[58] R.E. Bank, R.K. Smith, A posteriori error estimates based on hierarchical bases, SIAM J. Numer. Anal. 30 (1993) 921–935.
[59] P. Antolin, A. Buffa, L. Coradello, A hierarchical approach to the a posteriori error estimation of isogeometric Kirchhoff plates and Kirchhoff-Love shells, Comput. Methods Appl. Mech. Engrg. 363 (2020) 112919.
[60] L. Coradello, P. Antolin, R. Vázquez, A. Buffa, Adaptive isogeometric analysis on two-dimensional trimmed domains based on a hierarchical approach, Comput. Methods Appl. Mech. Engrg. 364 (2020) 112925.
[61] W. Dörfler, A convergent algorithm for Poisson's equation, SIAM J. Numer. Anal. 33 (1996) 1106–1124.
[62] J. Benzaken, J.A. Evans, S.F. McCormick, R. Tamstorf, Nitsche's method for linear Kirchhoff-Love shells: formulation, error analysis, and verification, Comput. Methods Appl. Mech. Engrg. 374 (2021) 113544.
[63] F. Cirak, M. Ortiz, Fully C^1-conforming subdivision elements for finite deformation thin-shell analysis, Internat. J. Numer. Methods Engrg. 51 (2001) 813–833.
[64] J. Kiendl, K.-U. Bletzinger, J. Linhard, R. Wüchner, Isogeometric shell analysis with Kirchhoff-Love elements, Comput. Methods Appl. Mech. Engrg. 198 (2009) 3902–3914.
[65] J. Kiendl, Isogeometric Analysis and Shape Optimization of Shell Structures (Ph.D. thesis), Technische Universität München, 2012.
[66] K.-J. Bathe, A. Iosilevich, D. Chapelle, An evaluation of the MITC shell elements, Comput. Struct. 75 (2000) 1–30.
[67] Y. Ko, P.-S. Lee, K.-J. Bathe, A new MITC4+ shell element, Comput. Struct. 182 (2017) 404–418.
[68] Y. Mi, X. Yu, Isogeometric MITC shell, Comput. Methods Appl. Mech. Engrg. 377 (2021) 113693.
[69] S. Bieber, B. Oesterle, E. Ramm, M. Bischoff, A variational method to avoid locking—independent of the discretization scheme, Internat. J. Numer. Methods Engrg. 114 (2018) 801–827.
[70] R.A. Sauer, Z. Zou, T.J.R. Hughes, A simple and efficient hybrid discretization approach to alleviate membrane locking in isogeometric thin shells, Comput. Methods Appl. Mech. Engrg. 424 (2024) 116869.